

Full Length Article

P2x7 receptors control demyelination and inflammation in the cuprizone model

Ana Bernal-Chico^{a,b,c,e}, Andrea Manterola^{a,b}, Raffaella Cipriani^{a,b}, István Katona^e,
Carlos Matute^{a,b,c,**}, Susana Mato^{a,b,c,d,*}

^a Department of Neurosciences, School of Medicine, University of the Basque Country UPV/EHU, 48940, Leioa, Spain

^b Achucarro Basque Center for Neuroscience, 48940, Leioa, Spain

^c Centro de Investigación Biomédica en Red sobre Enfermedades Neurodegenerativas (CIBERNED), 28031, Madrid, Spain

^d Biocruces, Bizkaia, 48903, Barakaldo, Spain

^e Momentum Laboratory of Molecular Neurobiology, Institute of Experimental Medicine, Hungarian Academy of Sciences, 1083, Budapest, Hungary



ARTICLE INFO

Keywords:

P2x7 receptors
Multiple sclerosis
Cuprizone
Inflammation
Microglia
De- and remyelination

ABSTRACT

The contribution of P2x7 receptors to multiple sclerosis remains controversial, as both detrimental and beneficial effects resulting from P2x7 receptor loss-of-function have been reported in autoimmune models of the disease. Here we investigated the relevance of P2x7 receptors to de- and remyelination in the cuprizone model of T cell-independent myelin degeneration. Primary demyelination was induced by administration of 0.3% cuprizone in the diet for 3 and 6 weeks. Remyelination was studied in mice treated with the P2x7 receptor antagonists Brilliant Blue G (BBG, 50 mg/Kg) and NJN-47965567 (30 mg/Kg) for 2 weeks following 6 weeks of cuprizone challenge. Toxic demyelination induced a robust up-regulation of P2x7 receptors mainly localized on microglial cells. In parallel, we measured increased expression of several NLRP3-inflammasome and M1 polarization-associated genes in demyelinated tissue. Notably, mice deficient in P2x7 receptors exhibited attenuated demyelination, reduced presence of M1 microglia and reactive astrocytes as well as blunted expression of pro-inflammatory genes in response to cuprizone feeding. Nevertheless, blockade of P2x7 receptors during the remyelination phase did not improve the extent of myelin recovery nor attenuated glial reaction and inflammation in damaged white matter. These findings suggest that P2x7 receptors drive T cell-independent inflammation and demyelination, but are not relevant to regenerative responses involved in myelin repair.

1. Introduction

Multiple sclerosis (MS) is the most common inflammatory disorder of the human central nervous system (CNS) and the leading cause of disability in young and middle-aged people in the developed world (Koch-Henriksen and Sørensen, 2010). Of unknown etiology, the disease has for many years been explained by a coincidence of environmental and genetic factors leading to the appearance of focal lesions with demyelination, inflammation and axon degeneration as the major pathogenic mechanisms that cause the clinical manifestations. Based on the analysis of pattern I and II actively demyelinating lesions, MS has traditionally been considered an autoimmune disease initiated by blood-derived T lymphocytes and monocytes that invade the CNS and destroy oligodendrocytes and myelin (Compston and Coles, 2008).

Conversely, early pattern III lesions exhibit widespread oligodendrocyte apoptosis and microglial activation outweighing humoral and cellular immune responses as well as mitochondrial alterations suggesting dysfunction in complex IV of the respiratory chain (Lucchinetti et al., 2000; Mahad et al., 2008). These observations have led to the alternative hypothesis that damage to oligodendrocytes is a primary event in MS evolution which may contribute to chronic inflammation through epitope spreading (Barnett and Prineas, 2004; Henderson et al., 2009). Irrespective of the primary trigger for demyelination, acute MS symptoms are often reversible during the initial relapsing-remitting course of the disease, although most of the patients enter a secondary progressive phase in which irreversible axonal degeneration causes persistent disability (Trapp and Nave, 2008). Remission in MS is largely dependent on the differentiation of oligodendrocyte precursor cells (OPCs) to

* Corresponding author. Department of Neurosciences, School of Medicine, University of the Basque Country UPV/EHU, 48940, Leioa, Spain.

** Corresponding author. Department of Neurosciences, School of Medicine, University of the Basque Country UPV/EHU, 48940, Leioa, Spain.

E-mail addresses: carlos.matute@ehu.eus (C. Matute), susana.mato@ehu.eus (S. Mato).

<https://doi.org/10.1016/j.bbih.2020.100062>

Received 20 January 2020; Received in revised form 22 March 2020; Accepted 22 March 2020

Available online 28 March 2020

2666-3546/© 2020 The Author(s). Published by Elsevier Inc. This is an open access article under the CC BY-NC-ND license (<http://creativecommons.org/licenses/by-nc-nd/4.0/>).

mature oligodendrocytes capable of myelin repair, a process facilitated by effective polarization of cytotoxic M1 microglia/macrophages to a regenerative M2 phenotype (Miron and Franklin, 2014; Patrikios et al., 2006).

Alterations in ATP homeostasis and the ensuing activation of the low affinity P2x7 receptors play central roles in the pathology of neuro-inflammatory disorders (Idzko et al., 2014; Sperlágh and Illes, 2014). The P2x7 receptor is a ligand-gated cation channel predominantly expressed on peripheral immune cells and resident microglia though it has also been detected in astrocytes, oligodendroglia and neurons (Kaczmarek-Hajek et al., 2018; Sperlágh et al., 2006; Zhang et al., 2014). Stimulation of P2x7 receptors causes ATP-dependent activation of the NLRP3 inflammasome and the eventual maturation and release of the potent pro-inflammatory cytokine interleukin-1 β (IL-1 β) from activated immune cells (Giuliani et al., 2017) at the same time that regulates T cell proliferation and activation (Baricordi et al., 1999; Yip et al., 2009). On the other hand, P2x7 receptors may also play important roles in regulating inflammatory and immune responses through its cytolytic activity. Prolonged opening of the P2x7 receptor channel allows massive Ca²⁺/Na⁺ influx and membrane depolarization leading to the activation of apoptotic or necrotic pathways in different cell types including microglia/macrophages (Brough et al., 2002; Humphreys et al., 2000) and T lymphocytes (Adriouch et al., 2007; Aswad et al., 2005; Kawamura et al., 2005), but also neurons and glia (Jun et al., 2007; Matute et al., 2007). Thus, activation of P2x7 results in a widespread and complex regulation of neuroinflammatory events *in vivo* with either reduced or exacerbated immune responses and toxicity depending on the precise inflammatory context.

Compelling evidence implicates P2x7 receptors in the pathogenesis of MS. A putative association of the P2x7 receptor gene with this illness is indicated by the most frequent expression of the gain-of-function T allele of the rs17525809 polymorphism of the receptor (Gu et al., 2015; Oyanguren-Desez et al., 2011). Activation of P2x7 receptors triggers oligodendrocyte cytotoxicity and P2x7 protein levels are elevated in normal-appearing axon tracts of MS patients pointing to the possibility that ATP signaling through P2x7 receptors may be enhanced in this disease (Matute et al., 2007; Wang et al., 2009). At the preclinical level, both increased and decreased P2x7 receptor levels have been reported in the experimental autoimmune encephalomyelitis (EAE) model of MS in which disease pathology mimics the T cell-mediated inflammatory responses (Grygorowicz et al., 2011; Matute et al., 2007). However, EAE studies in P2x7 null mice have led to conflicting results likely related to the complexity of P2x7 receptor signaling on the function of T cells. In this regard, P2x7 receptor deficiency attenuates responsiveness to EAE through mechanisms involving reduced astroglial activation (Sharp et al., 2008), but exacerbated expression of the disease has also been reported in P2x7 receptor knockout mice using this animal model (Chen and Brosnan, 2006; Witting et al., 2006). Notably, pharmacological antagonism of P2x7 receptors attenuates EAE disease (Matute et al., 2007). Nevertheless, the potential utility of P2x7 receptor antagonists in MS remains a matter of debate due to an incomplete understanding of the pathophysiological mechanisms driven by the activation of these receptors during EAE and the absence of studies in complementary animal models of the disease.

A significant gap in our current understanding of the pathophysiological role of P2x7 receptors in MS concerns their role as modulators of tissue damage and repair during primary demyelination. The copper chelator cuprizone causes dysfunction of mitochondrial complex IV resulting in the selective death of myelin-forming oligodendrocytes followed by myelin disruption, astrogliosis, microglia/macrophage activation and proliferation of NG2⁺ OPCs that enable remyelination after cuprizone is discontinued (Skripuletz et al., 2011). Unlike EAE pathology, demyelination induced by cuprizone is considered primarily independent of the peripheral immune system and exhibits cellular changes that resemble pattern III lesions in MS patients. Thus, the cuprizone model allows investigation of the effects of P2x7 receptors on myelin

damage and repair independent of the modulation of T lymphocyte functions.

In the present study, we found increased P2x7 receptor expression during cuprizone-induced demyelination associated with stronger P2x7 receptor-immunoreactivity in microglial cells. Induction of P2x7 receptor expression was accompanied to up-regulated tissue levels of several inflammatory genes associated to the activation of the NLRP3-inflammasome and to the polarization of microglia/macrophages to a M1 pro-inflammatory phenotype. Mice lacking P2x7 receptors were resistant to toxic demyelination and exhibited attenuated microglia and astrocytic reaction as well as reduced levels of pro-inflammatory genes in response to cuprizone feeding. However, transcriptional analyses in purified microglia suggest that P2x7 receptors do not control the polarization of these cells in demyelinated tissue. Pharmacological blockade of the P2x7 receptors using two structurally unrelated antagonists did not enhance the efficiency of remyelination nor attenuated glial reaction 2 weeks after discontinuation of the toxin. These results suggest the involvement of P2x7 receptor-mediated signaling in the mechanisms of primary demyelination and T cell-independent inflammation with the possible relevance of microglia and astrocytic pool of cells.

2. Methods

2.1. Mice and cuprizone treatment

Experimental demyelination was induced by feeding 8 week-old male C57BL/6 mice (Charles River) a diet containing 0.3% cuprizone (bis-cyclohexanone oxaldihydrazone; Sigma-Aldrich) mixed into milled chow (Altromin) for 3 or 6 weeks. Remyelination was studied in mice returned to normal chow for 2 weeks following a 6 weeks cuprizone challenge. Gene and protein expression analyses were carried out in mice sacrificed at different time-points by comparison to control mice treated with a standard diet. P2x7 knockout mice on a C57BL/6 background were obtained from breeding pairs housed in the animal facility of the University of the Basque Country-UPV/EHU.

To study the effect of P2x7 receptor antagonists during remyelination wild-type animals were placed on a cuprizone-containing or -free diet for 6 weeks. Untreated controls and four animals of the cuprizone-treated group were sacrificed on the last day of cuprizone intoxication to verify demyelination. The remaining cuprizone-treated mice were randomly assigned to experimental groups and received intraperitoneal (i.p.) injections of the P2x7 receptor antagonists Brilliant Blue G (BBG; 50 mg/Kg; Bio-Rad) and JNJ-47965567 [N-((4-(4-phenyl-piperazin-1-yl)tetrahydro-2H-pyran-4-yl)methyl)-2-(phenylthio)nicotinamide)] (30 mg/Kg; kindly provided by Janssen Research & Development) or their corresponding vehicle solutions. BBG was administered in 15% DMSO: 4.25% PEG 400: 4.25% Tween-80: 76.5% in saline (Bernal-Chico et al., 2015) every 48 h during the 2 weeks remyelination phase. The administration regimen every 48 h was established considering that at least 40 h are necessary to excrete the non absorbed drug (WHO, 1970). JNJ-47965567 was prepared in 30% SBE-beta-cyclodextrin in H₂O and administered to mice every 24 h (Bhattacharya et al., 2013; Jimenez-Pacheco et al., 2016). Administration of either drug was initiated at day 1 after cuprizone withdrawal. Mice were daily weighted during drug administration in order to adjust the corresponding doses and sacrificed 24 and 48 h after the last administration of JNJ-47965567 or BBG and their corresponding vehicles, respectively, to allow drug washout from brain tissue. Animals were maintained under standard laboratory conditions with food and water *ad libitum*. All animal procedures were carried out in compliance with the European Communities Council Directive of 22 September 2010 on the protection of animals used for scientific purposes (Directive 2010/63/EU) and were approved by the local ethical committee (Comité de Ética en Experimentación Animal, CEEA-UPV/EHU).

2.2. Analysis of BBG levels in brain tissue

BBG levels in brain samples were determined by spectrophotometry analysis as previously described (Díaz-Hernández et al., 2012; Peng et al., 2009). Briefly, brain tissue was collected from mice anesthetized with ketamine/xylazine (80/10 mg/Kg, i.p.) and transcardially perfused with PBS 24 h after the last BBG injection ($n = 3$). The tissue was homogenized with a Potter homogenizer followed by an ultrasonic converter. Levels of BBG in brain samples from chronically treated mice were determined according to calibration curves generated by adding known amounts of BBG to homogenized tissue from control mice that did not receive the P2x7 antagonist. Samples were quantified with a Synergy-HT microplate reader at the maximal absorbance of BBG (576 nm).

2.3. Flow cytometry

Mice were decapitated under isoflurane anaesthesia (IsoVet®, B Braun, Barcelona, Spain) and forebrain cells purified according to previously described procedures (Manterola et al., 2018). Briefly, brain tissue was dissected and placed in enzymatic solution (116 mM NaCl, 5.4 mM KCl, 26 mM NaHCO₃, 1 mM NaH₂PO₄, 1.5 mM CaCl₂, 1 mM MgSO₄, 0.5 mM EDTA, 25 mM glucose, 1 mM L-cysteine) with papain (2 U/mL) and DNase I (150 U/μL, Invitrogen, Carlsbad, CA, USA) for digestion at 37 °C for 15 min. After homogenization, tissue clogs were removed by filtering the cell suspension through a 40 μm nylon strainer to a 50 mL Falcon tube quenched by 5 mL of 20% heat inactivated fetal bovine serum in Hank's Balanced Salt Solution (HBSS, Thermo Fisher Scientific, Waltham, MA, USA). For further enrichment of microglia, myelin was removed by using Percoll gradients (GE Healthcare Europe GmbH, Barcelona, Spain). Then, each sample was layered with HBSS and centrifuged for 20 min at 200 x g. Collected cells were washed in HBSS by centrifuging at 200 x g for 5 min and pellet was resuspended in 500 μL of sorting buffer (25 mM HEPES, 5 mM EDTA, 1% BSA, in HBSS). Cell suspensions were incubated with fluorochrome conjugated antibodies to CD11b (FITC; 1:100) and CD45 (PE; 1:100) (BioLegend, San Diego, CA, USA). Fc receptor Blocking Reagent was added to prevent nonspecific antibody binding to Fc receptors. Microglia were sorted as CD11b⁺ cells with low CD45 expression (Szulzewsky et al., 2015) using a BD FACS Jazz (2B/4YG) cell sorter and analyser (BD Bioscience, San José, CA, USA). Cells were collected in lysis buffer (Qiagen, Hilden, Germany) containing 1% β-mercaptoethanol and stored at -80 °C until processing. RNA from FACS-sorted microglia was extracted using the RNeasy plus Micro Kit (Qiagen). We confirmed that we had isolated a relatively pure population of microglia by nanofluidic qPCR analysis for the expression of several cell-type specific markers (*Rbfox3*, *Aqp4*, *Pdgfra*, *Ly6G*, *Gpr34*, *P2ry12* and *Tmem119*) (Supplementary Fig. 1).

2.4. Real-time quantitative polymerase chain reaction (qRT-PCR) in brain samples

Mice anesthetized with ketamine/xylazine (80/10 mg/Kg, i.p.) were transcardially perfused with cold RNase Free phosphate buffer saline (PBS, Ambion®, Life Technologies - Thermo Fisher Scientific) for 30 s in order to remove blood cells from brain. A single coronal slice containing the corpus callosum was trimmed between levels 1 and -1 bregma (Paxinos and Franklin, 2012) using a David Kopf Instruments brain blocker. Total RNA was extracted with the RNeasy Mini kit (Qiagen) using the RNase-free DNase kit according to the manufacturer's recommendations (Invitrogen). First strand cDNA synthesis was carried out with reverse transcriptase Superscript™ III (Invitrogen) using random primers. Specific primers for *P2rx7* and *Mbp* were designed with the Primer Express software (Applied Biosystems - Thermo Fisher Scientific) and targeted to exon junctions to avoid amplification of contaminating genomic DNA. Primer sequences were as follows: mouse *P2rx7* forward 5'- GTT CAG GGA GGA ATC AT-3' and reverse 5'-TGA TGG GAC CAG CTG TCT AGG T-3; mouse *Mbp* forward 5'- GGG GCT CTG GCA AGG

TAC-3' and reverse 5'- GCC ATA ATG GGT AGT TCT CGT GT -3'. *Gapdh*, *Hprt1*, *Ppia* and *Actb* (primers from IDT Integrated DNA Technologies, Leuven, Belgium) were included as candidate reference genes for normalization purposes. Real-time qPCR was performed using SsoFast™ EvaGreen Supermix (Bio-Rad). Amplifications were run in a CFX96™ Real-Time System (Bio-Rad). Data normalization was carried out by geometric averaging of *Gapdh* and *Hprt1* according to results from the geNorm algorithm (<https://genorm.cmgg.be/>) (v.3.4 software). Relative gene expression data were determined by the $2^{-\Delta\Delta C_t}$ method.

2.5. Nanofluidic qPCR in brain samples and purified microglia

Following quality control of RNA samples (2100 Bioanalyzer, Agilent Technologies, Santa Clara, CA, USA), cDNA synthesis, pre-amplification and amplification steps were performed at the General Genomics Service of the UPV/EHU. For nanofluidic qPCR, the pre-amplified cDNA samples were measured with no reverse transcriptase and no template controls on 48.48 Dynamic Array chips and processed in the BioMark HD Real-Time PCR System (Fluidigm Corporation, San Francisco, CA, USA). We used commercial primers from IDT Integrated DNA Technologies or Fluidigm Corporation. Data pre-processing and analysis were completed using Fluidigm Melting Curve Analysis Software 1.1.0 and Real-time PCR Analysis Software 2.1.1 (Fluidigm Corporation) to determine valid PCR reactions. *Gapdh*, *Hprt1*, *Ppia* and *B2m* were included as candidate reference genes for normalization purposes. Data were corrected for differences in input RNA using the geometric mean of *Gapdh*, *Hprt1* and *Ppia* according to results from geNorm and Normfinder (<https://moma.dk/normfinder-software>) algorithms. Relative expression values were calculated with the $2^{-\Delta\Delta C_t}$ method.

2.6. Western blot analysis

Anesthetized mice were transcardially perfused with cold PBS containing 140 mM NaCl, 7.5 mM Na₂HPO₄ and 2.5 mM NaH₂PO₄ (pH 7.4) for 30 s and the brains were rapidly removed. A single brain slice between levels 1 and -1 bregma was obtained from each mouse and homogenized (1:20 w/v) in ice-cold buffer (10 mM HEPES, 10 mM KCl, 1 mM MgCl₂, 1 mM DTT, pH 7.9) containing a protease inhibitor cocktail (Complete™, Mini EDTA-free tablets, Roche Diagnostics) by using a Potter homogenizer provided with a loosely fitting Teflon pestle. Samples were subjected to centrifugation (3,500 x g at 4 °C for 4 min) to remove insoluble material. Supernatants were removed and lysed by incubation in homogenization buffer containing 1% Triton X-100 for 30 min on ice. Solubilized proteins corresponding to the membrane and cytosolic fractions were recovered in the supernatants after centrifugation (18,000 x g for 10 min at 4 °C) and quantified using the Bio-Rad Protein Assay. Protein samples (10-15 μg) were loaded into polyacrylamide Criterion TGX Precast (Bio-Rad) gels before electrophoretic transfer onto PVDF membranes (Trans-Blot Turbo transfer pack, Midi Format 0.2 μm, Bio-Rad). Membranes were blocked for 1 h in Tris-buffered saline (TBS) (50 mM Tris, 200 mM NaCl, pH 7.4) with 0.05% Tween-20, 5% BSA and 1% normal goat serum. Subsequently, membranes were incubated overnight at 4 °C with primary antibodies anti-P2x7 receptors (1:1000; Alomone Labs; cat. no APR-004), anti-myelin basic protein (MBP; 1:5000; Millipore) and anti-β-actin (1:5000; Sigma-Aldrich, cat. no A2066). Membranes were incubated with horseradish peroxidase-conjugated secondary antibodies (1:5000; Cell Signaling Technology) and developed with Pierce ECL Western Blotting Substrate (Thermo Fisher Scientific). Volumetric analysis of relevant immunoreactive bands was carried out after acquisition on a ChemiDoc XRS System (Bio-Rad) controlled by the Quantity One software v 4.6.3 (Bio-Rad).

2.7. Histology, immunohistochemistry and image analysis

For histological examination anesthetized mice were transcardially perfused with 0.1 M phosphate buffer (25 mM NaH₂PO₄•H₂O; 75 mM

Na_2HPO_4 ; pH 7.4) followed by 4% paraformaldehyde (PFA) in the same buffer. After extraction, the brains were post-fixed in 4% paraformaldehyde for 4 h. Tissue samples for cryostat sectioning were cryoprotected overnight in 20% sucrose at 4 °C, embedded in Tissue-Tek OCT (Electron Microscopy Sciences) and stored at -80 °C until use. All histological analyses were carried out in serial coronal sections between levels 1 and -1 bregma as defined in the mouse brain atlas of Paxinos and Franklin (2012).

Demyelination and glial reactions were evaluated in 10 μm -thick cryostat sections using Luxol Fast Blue (LFB) and immunofluorescence standard protocols. Sections were rinsed and blocked for 60 min in TBS (100 mM Tris Base, 150 mM NaCl; pH 7.4) supplemented with 5% normal goat serum and 0.1–0.2% Triton X-100. For MBP immunolabelling tissue sections were permeabilized in methanol at -20 °C for 10 min prior to blocking. Primary antibody incubation was carried out overnight at 4 °C using specific antibodies against MBP (1:1000; Covance; cat. no. SMI-99P), GFAP (1:40; Millipore; cat. no. MAB3402) for astrocytes, CD11b (1:100; Millipore; cat. no. MAB1387Z) or Iba1 (1:1000; Wako; cat. no. 019-19741) for microglia/macrophages, NG2 (1:200; Millipore; cat. no. AB5320) for OPCs, CD3 (1:50; Serotec; cat. no. MCA1477) for T cells, MAC387 (1:50; Santa Cruz; cat. no. sc-66204) for infiltrating peripheral blood monocytes, and myeloperoxidase (MPO; 1:40; Abcam; cat. no. ab9535) for granulocytes/neutrophils.

For the quantification of demyelination and glial reaction, optical images from tissue sections processed in parallel were acquired in the same session using a Zeiss Axioplan 2 microscope coupled to an AxioCam MRC5 digital camera (Zeiss). Myelin damage was blind scored by two observers in LFB or MBP stained sections using a 5-point scale ranging from 4 (normal myelin) to 0 (complete demyelination). Glial reactivity and immune cell infiltration were evaluated in two coronal sections per mouse separated 200 μm by examination of two digital 40X objective pictures including the middle line of the corpus callosum obtained from each slice. In all cases, analyses of immunostained sections was carried out using microscope fluorescence intensity settings at which the control sections without primary antibody gave no signal. Immunoreactivity was quantified using NIH Image J Software. Threshold analysis of GFAP immunostained area was carried out in 16-bit grey scale transformed pictures and the values were referred to the total corpus callosum area in each optical section. CD11b, Iba1, NG2, CD3, MAC387 and MPO-positive cells were quantified by cell counting and data expressed as mean cell number per square millimetre of corpus callosum area.

Double immunolabelling of vibratome sections was used to investigate the localization of P2x7 receptors and to examine the phenotype of microglia in the demyelinated corpus callosum of cuprizone-treated mice. Free-floating 40 μm sections were rinsed in TBS (pH 7.4) and incubated for 60 min at RT in a blocking-permeabilization solution containing 1% human serum (HSA) (Vector Laboratories) and 0.3% Triton X-100 in TBS. Sections were incubated for 30 min at RT and 48 h at 4 °C with a combination of primary antibodies against P2x7 receptors (1:1000; Alomone Labs; cat. no. APR-004), GFAP (1:500; Millipore; cat. no. MAB3402), CD11b (1:500; Millipore; cat. no. MAB1387Z), iNOS (1:100; Abcam; cat. no. ab129372) or Arg-1 (1:50; Santa Cruz Biotechnology; cat. no. sc-18355) diluted in TBS supplemented with 0.1% Triton X-100. Following extensive washing, primary antibodies were detected by incubation with appropriate Alexa Fluor 488 or 594 conjugated donkey antibodies (1:400; Invitrogen) for 1–2 h at room temperature. Hoechst 33258 (5 $\mu\text{g}/\text{ml}$; Sigma-Aldrich) was used for chromatin staining. Sections were mounted in Vectashield (Vector Laboratories; H1000) mounting medium. Tissue sections from P2x7 receptor knockout mice processed in parallel were used as internal control for the specificity of the immunostaining (Supplementary Fig. 2). Immunofluorescence controls were routinely performed with incubations in which primary antibodies were not included. Confocal microscopy of dual-labelled tissue sections was performed using a Leica TCS Sp8X STED CW confocal laser scanning microscope. Series of optical sections (z-stacks) were taken through the corpus callosum at a spacing of 0.3 μm using a 40X oil

immersion objective. For the analysis of microglia phenotype, localization of iNOS and Arg-1 in CD11b⁺ cells was examined in z-stacks. Threshold analysis of P2x7 receptor immunostained area in the corpus callosum was carried out in single confocal planes acquired at 5 μm from tissue surface using NIH Image J Software as described above. The expression of P2x7 receptor in glial cells was evaluated by examination of the z-stacks taken through dual-labelled tissue sections. For quantitative analysis of P2x7 receptor localization in glial cells, frequency distributions of fluorescent intensities from green and red fluorochromes were presented as scatter plots and colocalization rates and Pearson's coefficients analyzed using the proprietary Leica Confocal LAS-AF Software (v 3.3.0.10134).

2.8. Data analysis

Data are presented as mean \pm SEM and *n* represents the number of animals tested. Data were analyzed with Microsoft Excel and GraphPad Software by means of Student's *t* test and one-way ANOVA followed by Newman-Keuls multiple comparison tests, with *p* values < 0.05 considered statistically significant.

3. Results

3.1. Increased P2x7 receptor expression and signalling during demyelination by cuprizone feeding

Previous studies have reported either increased or decreased levels of P2x7 receptors in the T cell-dependent EAE model of MS (Grygorowicz et al., 2011; Matute et al., 2007). However, the expression pattern of P2x7 receptors in animal models of primarily T cell-independent de- and remyelination remains uncharacterized. Thus, we first evaluated whether *P2rx7* gene expression and protein levels are altered in response to cuprizone feeding. Exposure to a cuprizone containing diet for 3 and 6 weeks induces effective demyelination of the forebrain as reflected by the progressive decline in the expression of myelin genes and proteins in the corpus callosum (Manterola et al., 2018). Accordingly, we measured decreased expression of *Mbp* transcripts following 3 weeks of toxin feeding paralleled by a decline at the protein level that persisted until 6 weeks (Fig. 1A–B). *P2rx7* gene expression was markedly up-regulated during the course of demyelination with a maximal induction of 5-fold at 3 weeks of cuprizone feeding (Fig. 1A). This early transcriptional response was associated with a more progressive up-regulation of the P2x7 receptor protein with significant 2.5-fold increases measured by western blot at 6 weeks of treatment (Fig. 1B). At this time-point P2x7 receptor expression was specifically increased in demyelinated corpus callosum as primary focus of cuprizone-induced demyelination, as confirmed by immunohistochemistry (Fig. 1C). To evaluate changes in P2x7 receptor expression during remyelination, mice were treated with cuprizone for 6 weeks and returned to control diet for 2 weeks. Removal of cuprizone at 6 weeks led to spontaneous remyelination 2 weeks later as evidenced by the up-regulation of *Mbp* transcripts and MBP protein expression to levels similar to or slightly above than untreated age-matched controls (Fig. 1A–B). The transcriptional *Mbp* response associated to myelin repair was paralleled by the normalization of *P2rx7* transcripts to control levels 2 weeks after cuprizone removal (Fig. 1A). Notably, western blot analysis showed that P2x7 receptor levels remained 1.8-fold elevated at this point of the remyelination phase (Fig. 1B). Altogether, these data indicate a dynamically regulated increase in P2x7 receptors during primary demyelination and remyelination.

Next, we sought for possible changes in the expression of P2x7 signaling related molecules at the time of maximal receptor up-regulation by cuprizone feeding. Functionally, the P2x7 receptor chiefly acts through the recruitment of the NLRP3 inflammasome-caspase-1 complex to produce pro-inflammatory IL-1 β and IL-18 in peripheral and resident immune cells (Giuliani et al., 2017). Consistently, we measured increased

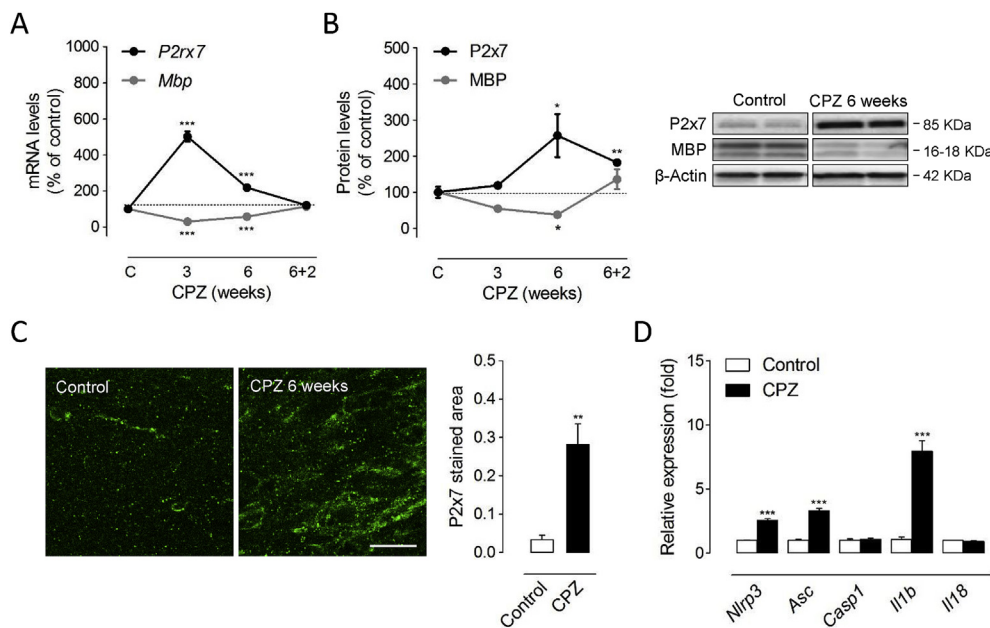


Fig. 1. Up-regulated P2x7 receptor expression and signalling during cuprizone intoxication. (A) RT-qPCR analyses showed significant increases in *P2rx7* expression during the time-course of cuprizone administration ($n = 7$ mice per group; normalized to *Gapdh* and *Hprt1*). (B) Up-regulated P2x7 receptor levels were detected following 6 weeks of cuprizone feeding ($n = 5$ mice per group). At each treatment point, brain slices from cuprizone-treated mice were compared with tissue from mice fed a control diet. (C) Representative images of P2x7 receptor immunostaining in the corpus callosum of mice treated with a cuprizone containing diet for 6 weeks and untreated controls. Quantification of immunolabelled tissue sections revealed significant up-regulation of P2x7 receptors in demyelinated corpus callosum ($n = 4$ mice per group). (D) Increased expression of inflammasome-related molecules following 6 weeks of cuprizone intoxication. Transcript levels of indicated genes were assessed by RT-qPCR. Data represent relative fold change compared with controls normalized to *Gapdh*, *Hprt1* and *Ppia* ($n = 4-5$ mice per group). CPZ, cuprizone. * $p < 0.05$, ** $p < 0.01$ and *** $p < 0.001$ referred to the control groups, Student's *t* tests. Scale bars: 20 μ m.

gene expression of inflammasome-related genes *Nlrp3*, *Asc* and *Il1b* in brain tissue at 6 weeks of cuprizone feeding (Fig. 1D). Together, these observations suggest that P2x7 receptor-mediated signalling regulates the cellular and biochemical events that orchestrate demyelination by cuprizone feeding.

3.2. P2x7 receptor deficiency attenuates demyelination and inflammation

To further investigate the contribution of P2x7 receptors to the events governing primary demyelination we took advantage of P2x7 receptor deficient mice. Wild-type and P2x7 receptor knockout mice treated in parallel were examined following 6 weeks of cuprizone administration, matching the time point of maximal P2x7 receptor up-regulation. Histological evaluation evidenced attenuated myelin loss in the corpus callosum of P2x7 receptor deficient mice (Fig. 2A). The depletion of mature oligodendrocytes by cuprizone intoxication is associated with a prominent inflammatory reaction consisting in the large accumulation of microglia and astrocytes, paralleled by the accumulation of OPCs responsible for myelin repair (Skripuletz et al., 2011). Thus, we next examined whether the reduced susceptibility of P2x7 receptor knockout mice to cuprizone-induced demyelination was associated with specific cellular changes. Immunolabelling of CD11b and GFAP revealed reduced numbers of microglial cells and attenuated astrocytic reaction in demyelinated corpus callosum of P2x7 deficient mice (Fig. 2B). By contrast, we detected no differences between wild-type and P2x7 knockout animals regarding the recruitment of NG2⁺ OPCs upon cuprizone-induced myelin loss (Fig. 2C). We also evaluated possible changes between genotypes regarding the infiltration of peripheral immune cells during cuprizone intoxication. To this end, we stained T cells, recently infiltrating monocytes/macrophages and neutrophils by using antibodies against CD3, MAC387 and MPO, respectively. Although T cells were rarely detected in the corpus callosum of 6 week cuprizone-treated mice, we quantified low numbers of infiltrating monocytes/macrophages and neutrophils in wild-type mice that were not modulated by P2x7 receptor deficiency (Fig. 2D). These data suggest that P2x7 contributes to demyelination by cuprizone feeding without OPC or peripheral cell involvement.

Finally, we investigated whether the myelin protective phenotype of

P2x7 receptor null mice was associated to a blunted activation of the NLRP3 inflammasome complex. Profiling of brain transcript levels at 6 weeks of cuprizone-feeding showed attenuated induction of several inflammasome-associated genes including *Asc*, *Casp1* and *Il1b* in P2x7 receptor null mice (Fig. 2E). Altogether, these results suggest that activation of P2x7 receptors upstream the NLRP3 inflammasome complex promotes demyelination and inflammation in the cuprizone model.

3.3. Localization of P2x7 receptors in demyelinated corpus callosum

We next aimed at determining the cellular substrates of P2x7 receptor up-regulation and signaling during cuprizone feeding. Because P2x7 null mice exhibited attenuated accumulation of microglia and astrocytes in demyelinating white matter and both cell types are possible targets for P2x7 receptor mediated signaling during neuroinflammation (Sperlgh and Illes, 2014), we conducted double immunolabelling studies using antibodies for P2x7 receptors and either CD11b or GFAP to specifically label each cell population. High magnification confocal microscopy suggested a predominant P2x7 receptor expression by the microglial cell population in injured white matter, as the majority of P2x7 receptor immunostaining appeared to lie on cell bodies and processes positive for the microglia/macrophage marker CD11b (Fig. 3A). We also detected scattered P2x7 receptor puncta in potential association with the intracellular marker GFAP, which visualizes mainly astrocytic profiles (Fig. 3B). We confirmed these observations by cytofluorogram analysis of P2x7/CD11b and P2x7/GFAP colocalization in double-labelled tissue sections, which yielded higher colocalization rates and Pearson's coefficients when pixel intensity for P2x7 receptors was plotted against CD11b (Fig. 3C-D). This predominant distribution in microglia versus astrocytes is in good agreement with previous localization and RNA sequencing data in non-injured grey matter (Kaczmarek-Hajek et al., 2018; Zhang et al., 2014). Finally, comparison of both colocalization parameters between mice fed cuprizone or control diet revealed that administration of the toxin was associated to a selective up-regulation of P2x7/CD11b colocalization values (Fig. 3C-D). Collectively, these results indicate that P2x7 receptor overexpression resulting from demyelination of the corpus callosum is preferentially related to the microglia versus astrocytic pool of inflammatory cells.

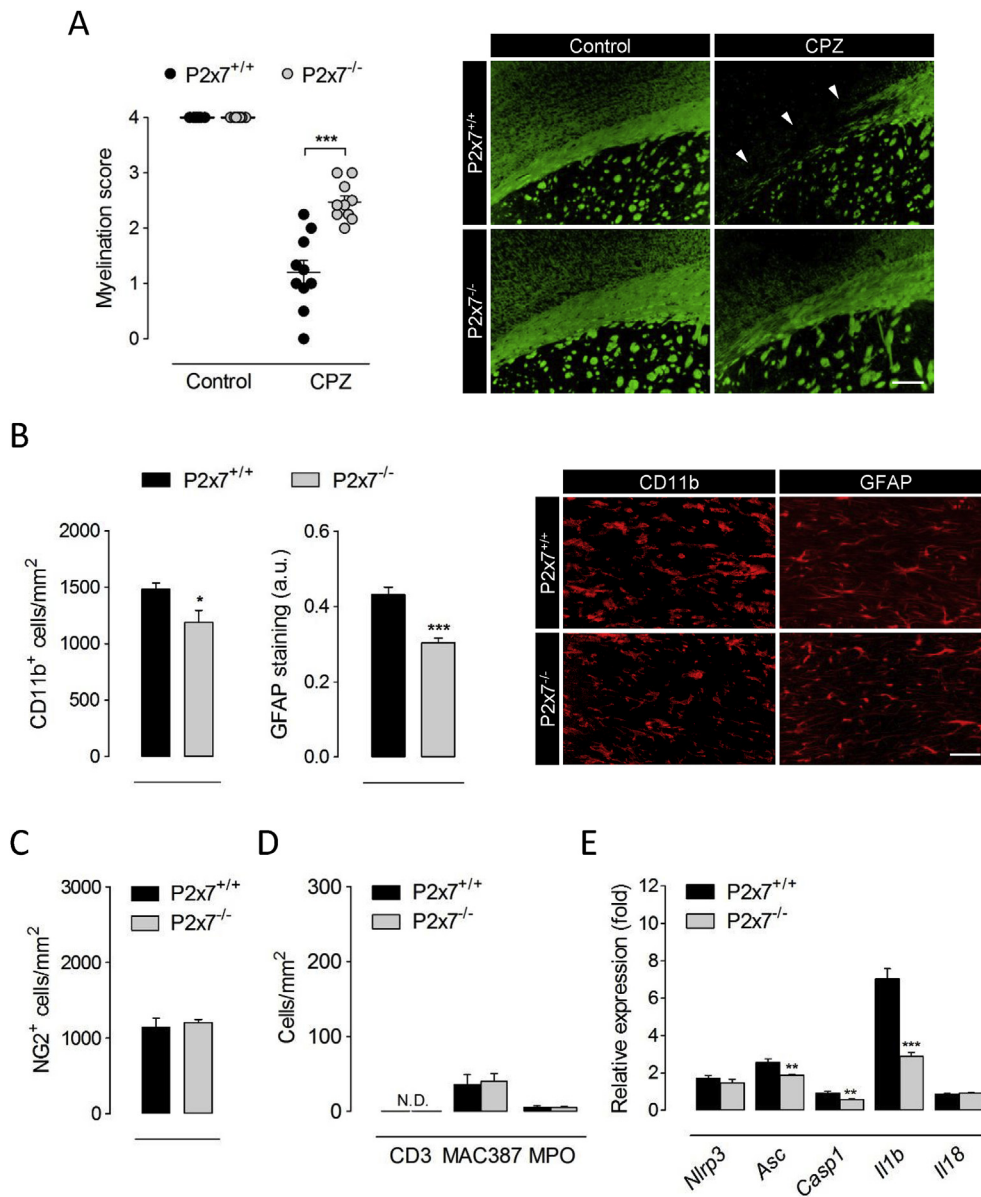


Fig. 2. P2x7 receptor deficient mice are resistant to cuprizone-induced demyelination. (A) P2x7^{+/+} and P2x7^{-/-} mice were fed 0.3% cuprizone in the diet for 6 weeks. Analysis of tissue sections stained for LFB and MBP showed attenuated myelin loss in P2x7 receptor deficient mice ($n = 3-5$ mice). Representative images depict the loss of MBP immunolabelling after cuprizone administration in P2x7^{+/+} and P2x7^{-/-} mice. (B-D) The corpus callosum was immunostained for CD11b, GFAP, NG2, CD3, MAC387 and myeloperoxidase (MPO) as markers of microglia/macrophages, astrocytes, OPCs, T cells, recently infiltrating monocytes/macrophages and neutrophils, respectively. Quantification and representative images show a reduced accumulation of astrocytes and microglia in P2x7^{-/-} mice at 6 weeks of cuprizone diet (B), but no differences regarding the recruitment of OPCs (C) or peripheral immune cells (D) to demyelinated tissue ($n = 4-5$ mice). (E) Transcript levels of inflammasome-associated genes were assessed by RT-qPCR in brain tissue from P2x7^{+/+} and P2x7^{-/-} mice at 6 weeks of cuprizone intoxication. Data represent relative fold change compared with controls normalized to *Gapdh*, *Hprt1* and *Ppia* ($n = 4-5$ mice per group). Scale bars: 200 μ m (A) and 50 μ m (B). CPZ, cuprizone; N.D., not detected. * $p < 0.05$, ** $p < 0.01$ and *** $p < 0.001$ referred to the control groups, Student's t tests.

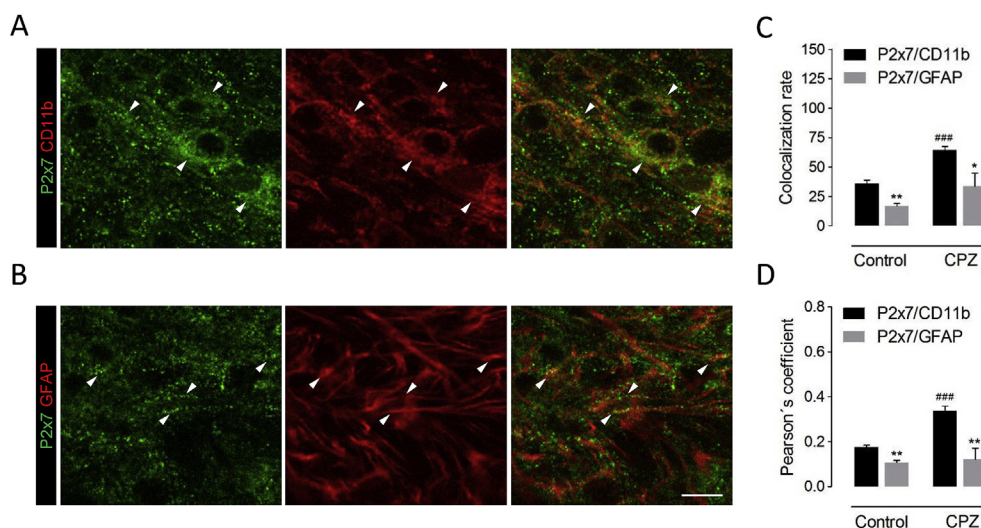


Fig. 3. Cell-specific analysis of P2x7 receptor expression in cuprizone-treated mice. Confocal images corresponding to double immunostaining of P2x7 receptors and the microglia/macrophage marker CD11b (A) and the astrocytic marker GFAP (B) in the corpus callosum of mice fed a cuprizone containing diet for 6 weeks. (C-D) Analysis of confocal fluorescent images indicated higher colocalization of P2x7 receptor immunopositive puncta with CD11b⁺ microglia than with GFAP⁺ astrocytic profiles, both in control and in cuprizone-treated mice ($n = 4$ mice per group). CPZ, cuprizone. * $p < 0.05$ and ** $p < 0.01$ versus P2x7/GFAP colocalization; *** $p < 0.001$ versus untreated controls; Student's t tests. Scale bar: 10 μ m.

3.4. P2x7 receptors favour the accumulation of pro-inflammatory microglia in demyelinated tissue

Activated microglial cells can be phenotypically polarized to develop a classical pro-inflammatory phenotype (M1), an alternative, anti-inflammatory and prohealing (M2) phenotype, or acquire intermediate functional phenotypes that display combinations of different M1/M2 polarization markers (Hu et al., 2015). The nature of microglia polarization has recently emerged as a key determinant of demyelination, with M1 cells promoting white matter damage and M2 dominant responses preventing oligodendrocyte loss and enabling repair (Chu et al., 2018; Guglielmetti et al., 2016; Le Blon et al., 2016; Miron et al., 2013; Yu et al., 2015). In this context, we sought to investigate the role of P2x7 receptors as regulators of microglia phenotype during primary demyelination. To this end, we first analyzed the functional polarization of microglia at the transcriptional level using a variety of M1- and M2-associated markers (Chu et al., 2018). The expression of several M1 signature genes, namely *Cd86*, *Cybb*, *Lyz2*, *Stat1*, *Tnfa*, *Ccl2* and *Ccl3*, was markedly increased in brain tissue from mice receiving a cuprizone containing diet for 6 weeks (Fig. 4A). By contrast, M2-related markers were either not regulated (*Mrc1*, *Arg1*, *Stat6* and *Jak3*) or only modestly increased (*Cd163* and *Chil3*) upon cuprizone intoxication (Fig. 4A). These results are in line with previous reports showing a preferential induction of M1 signature microglia upon demyelination by cuprizone feeding (Aryanpour et al., 2017; Chen et al., 2014; Duan et al., 2018). We next tested the contribution of P2x7 receptors to the expression of microglia activation markers by challenging P2x7 receptor knockout mice with a cuprizone diet. Of note, mice lacking P2x7 receptors showed attenuated expression of most M1 phenotype markers up-regulated in demyelinated tissue, but no changes regarding M2 signature genes (Fig. 4B). To corroborate these observations we evaluated microglia polarization at the translational level using double immunofluorescence for CD11b together with iNOS or Arg-1 as M1 and M2 phenotype markers, respectively (Miron et al., 2013). Consistent with transcriptional studies, quantification of immunofluorescent images indicated a predominant expression of iNOS⁺ in the CD11b⁺ cell population in demyelinated corpus callosum with only a small percentage of microglial cells displaying Arg-1⁺ immunostaining in wild-type and P2x7 deficient mice (Fig. 4C-D). Furthermore, P2x7 knockout mice exhibited a slight but significant reduction in the presence iNOS⁺/CD11b⁺ cells as compared to wild-type animals, while the number of Arg-1⁺/CD11b⁺ cells was similar between the two groups (Fig. 4C-D). In all, these results suggest that P2x7 receptors promote microglia switching to a pro-inflammatory phenotype during cuprizone-induced demyelination.

3.5. Microglia polarization to a pro-inflammatory phenotype is not under the control of P2x7 receptors

To further explore the hypothesis that P2x7 receptors modulate microglial inflammasome activation and polarization during primary demyelination we carried out gene expression analyses in cells purified from wild-type and P2x7 receptor null mice at 6 weeks of cuprizone intoxication. Unexpectedly, *P2rx7* mRNA levels were slightly down-regulated in microglia from cuprizone-treated mice (Fig. 5A). This result is in apparent contrast to the observed up-regulation at the protein level (Fig. 3), but in agreement with previous reports showing reduced *P2rx7* transcripts in mouse microglia under long-lasting pro-inflammatory conditions (He et al., 2017). Supporting activation of the NLRP3 inflammasome, demyelination-associated microglia displayed increased levels of the pro-inflammatory cytokine *Il1b* (Fig. 5A). However, additional inflammasome-related genes were either unaltered (*Nlrp3* or *Asc*) or down-regulated (*Il18*) (Fig. 5A). Similarly, most M1 signature genes displayed either unchanged (*Nos2*, *Stat1*, *Tnfa* and *Ccl3*) or even diminished (*Cd86*, *Il6* and *Ccl2*) expression in microglia purified from cuprizone-treated mice, although we also measured up-regulated expression of several pro-inflammation markers, namely *Cybb*, *Ptgs2* and

Lyz2 (Fig. 5C). On the other hand, demyelination-associated microglia displayed significant down-regulation of all the M2 phenotype genes tested (*Cd163*, *Mrc1*, *Stat6* and *Jak3*) (Fig. 5C). Overall, these data are generally consistent with our observations in brain tissue (Fig. 4A-D) and support the hypothesis that microglia activated during demyelination exhibit a dominant pro-inflammatory phenotype. Our findings also indicate that the inflammatory signature of demyelinated tissue at the gene expression level does not faithfully mirror changes in the transcriptomic profile of microglial cells. In this context, the observed up-regulation of NLRP3 inflammasome- and M1-associated genes in brain samples from cuprizone treated mice is likely to reflect, at least in part, changes in the gene expression signature of additional cell types, likely astrocytes, as well as the net increase in the numbers of inflammatory cells in injured tissue. Noteworthy, microglia purified from P2x7 receptor null mice at 6 weeks of cuprizone intoxication did not exhibit changes in the expression of inflammasome activation- and M1/2 polarization-related genes (Fig. 5B, D). These results indicate that signaling through P2x7 receptors does not drive the phenotypical polarization of microglia at the time-point of maximal demyelination by cuprizone.

3.6. In vivo antagonism of P2x7 receptors does not accelerate myelin repair

Although previous data have established a proof of principle that P2x7 receptor antagonists can reduce the severity of EAE (Matute et al., 2007) the potential ability of these compounds to promote myelin repair has not been specifically addressed. Thus, we next explored the therapeutic benefit of P2x7 receptor blockade during the remyelination phase of cuprizone induced myelin degeneration. With this aim we used the P2x7 receptor antagonist BBG (Jiang et al., 2000) under a dose regimen that effectively attenuates brain pathology in rodent models of Alzheimer's and Huntington's diseases (Diaz-Hernandez et al., 2012; Díaz-Hernández et al., 2009). Mice treated with cuprizone for 6 weeks were randomly assigned to treatment groups and administered BBG or vehicle every 48 h over a 2 week interval starting at day 1 after toxin withdrawal. Levels of BBG in brain homogenates from chronically treated mice averaged 378 ± 0.17 nM (see Materials and Methods), thus in the range of the IC₅₀ of BBG to antagonize P2x7 receptors (10–200 nM) (Jiang et al., 2000). Analysis of tissue sections stained for LFB and MBP showed significant improvement of myelination scores 2 weeks after cuprizone removal in both treatment groups (Fig. 6A). Nevertheless, the degree of remyelination was similar between vehicle and BBG treated mice. We further assessed remyelination by qPCR analysis of *Mbp* expression in the same animals. Consistent with our histopathological observations, comparison of BBG and vehicle-treated mice revealed no effect of drug administration on *Mbp* levels over the recovery interval (Supplementary Fig. 3A). To confirm these results, we tested the effect of a structurally unrelated P2x7 receptor antagonist in an independent remyelination experiment. As described for BBG administration, mice treated with the brain penetrating compound JNJ-47965567 (Bhattacharya et al., 2013) showed no significant improvement in the extent of myelin recovery at the experimental end-point, as determined by immunohistochemistry (Fig. 6B) and *Mbp* expression analysis (Supplementary Fig. 3A). Lastly, treatment with either P2x7 receptor antagonist did not accelerate body weight recovery during the remyelination phase (Supplementary Fig. 3B).

Because we localized P2x7 receptors on microglia and astrocytes of the demyelinated corpus callosum (Fig. 3), we next evaluated the effect of BBG and JNJ-47965567 treatment over the 2 week recovery phase on these cell types. We did not detect significant modifications between vehicle and drug-treated mice concerning the number of cells positive for the microglial/macrophage markers CD11b and Iba1, or the extent of GFAP immunostaining in remyelinating white matter (Fig. 7A). Finally, we analyzed the effect of BBG and JNJ-47965567 on the expression of inflammasome- and polarization-related genes in brain tissue. Mice

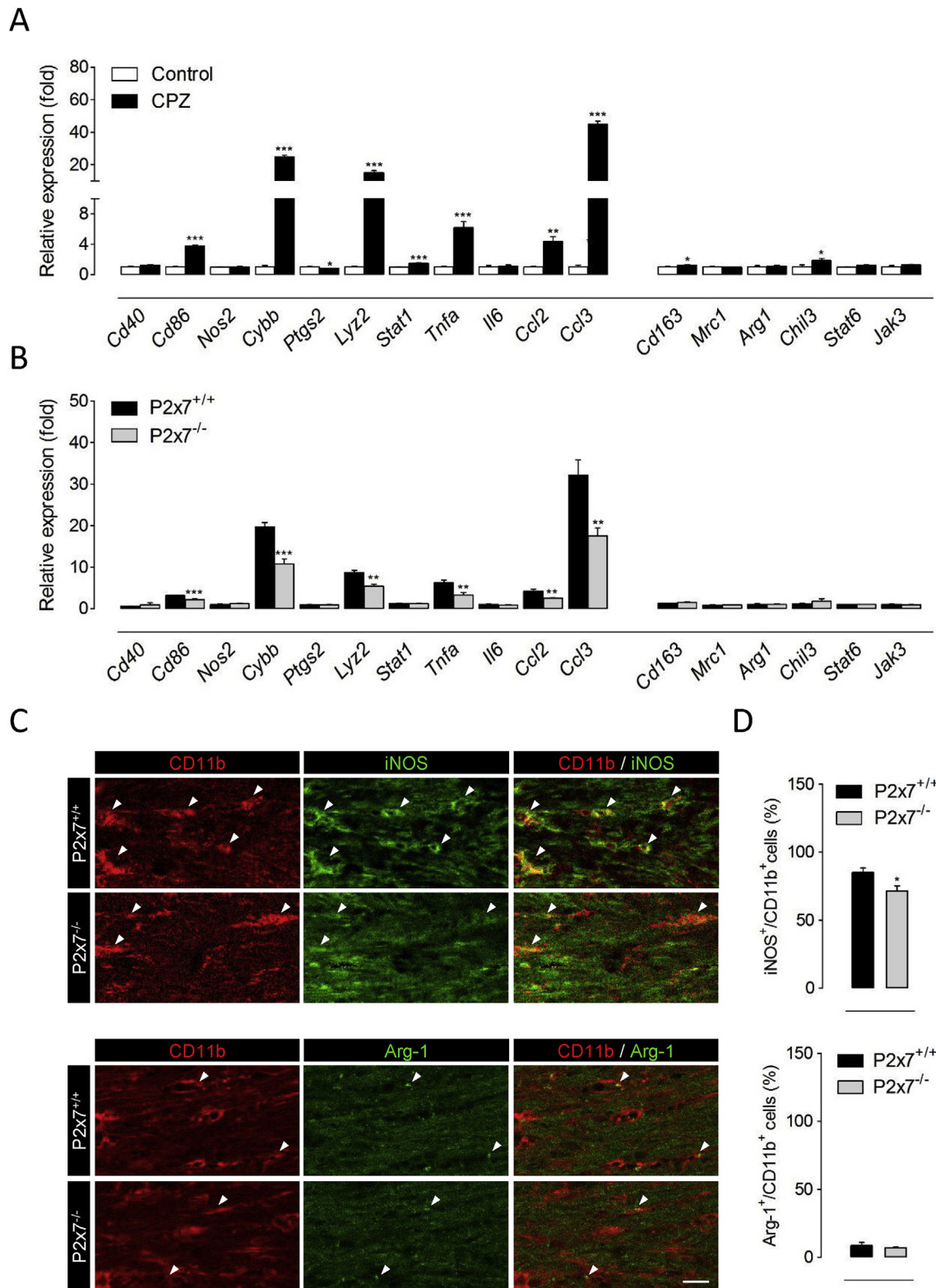


Fig. 4. P2x7 receptors promote the accumulation of pro-inflammatory microglia during cuprizone-induced demyelination. (A) RT-qPCR analysis of M1 and M2 signature genes in brain tissue from mice treated with a cuprizone-containing diet for 6 weeks. Data represent relative fold change compared with controls normalized to *Gapdh*, *Hprt1* and *Ppia* ($n = 4-5$ mice per group). (B) P2x7 knockout mice displayed down-regulated induction of M1 phenotype markers at 6 weeks of cuprizone intoxication. Results are expressed as relative fold change relative to controls normalized to *Gapdh*, *Hprt1* and *Ppia* ($n = 6$ mice per group). (C-D) Quantification and representative images depicting iNOS and Arg-1 colocalization with CD11b in mice treated with cuprizone for 6 weeks. P2x7^{-/-} mice exhibited a significant reduction in the number of CD11b⁺ cells expressing iNOS in demyelinated corpus callosum. Scale bars: 20 μ m. CPZ, cuprizone. * $p < 0.05$, ** $p < 0.01$ and *** $p < 0.001$ referred to the control groups, Student's t tests.

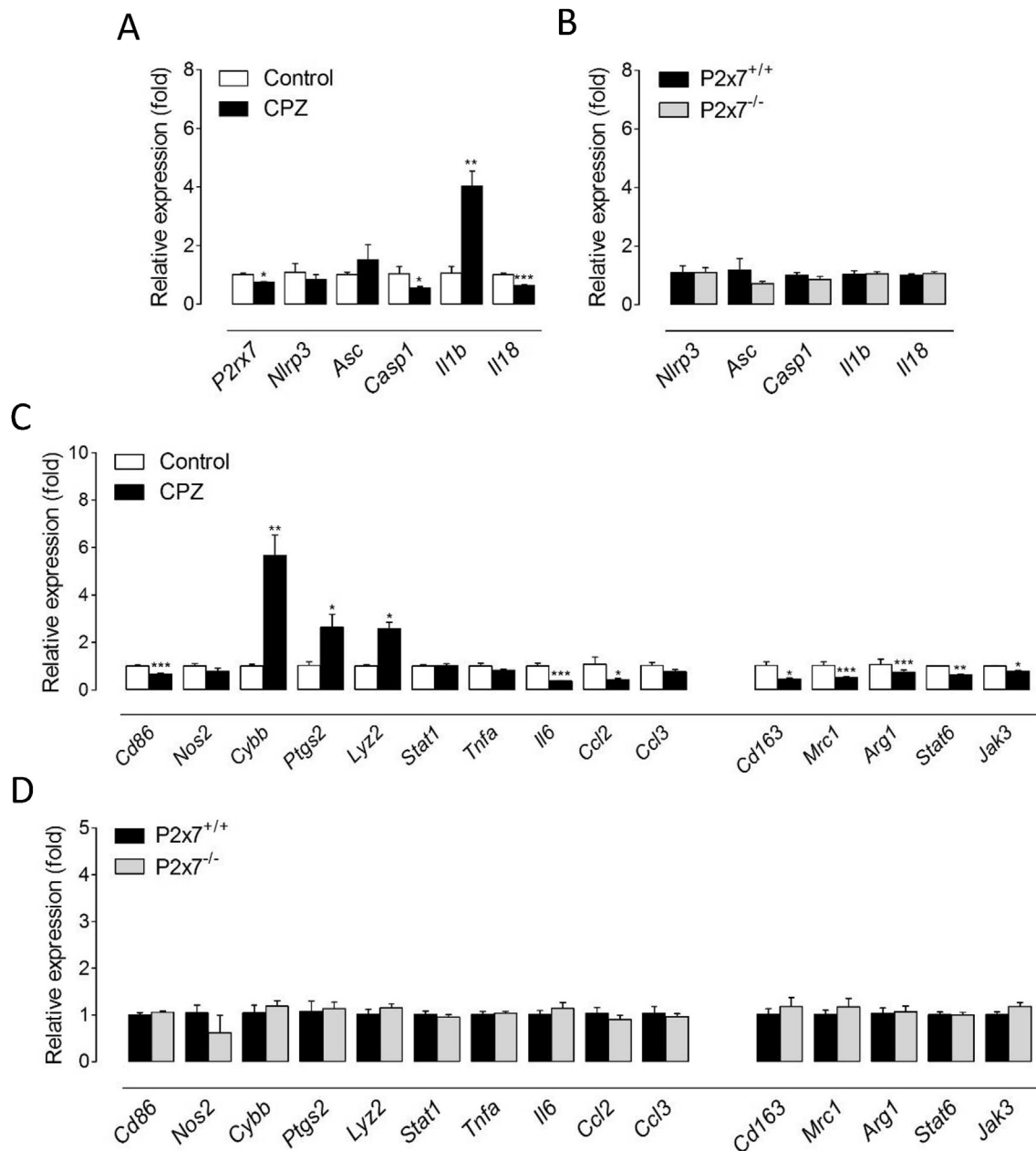


Fig. 5. P2x7 receptors are not master regulators of demyelination-associated microglia phenotype. Wild-type and P2x7 knockout mice were treated with cuprizone for 6 weeks and microglial cells purified from the forebrain using flow cytometry. RT-qPCR analysis of inflammasome activation markers (A) and M1/M2 phenotype genes (C) in cell sorted from control and cuprizone-treated mice showed selective up-regulation of several pro-inflammatory genes in demyelination-associated microglia. Data represent relative fold change compared with microglial cells purified from control mice normalized to *B2m* and *Ppia* ($n = 3-6$ mice per group). (B, D) Relative expression of indicate genes in microglia sorted from cuprizone-treated P2x7 knockout mice ($n = 3-6$ mice per group; fold change compared with expression levels in cells purified from cuprizone-treated wild-type mice; normalized to *B2m* and *Ppia*). CPZ, cuprizone. * $p < 0.05$, ** $p < 0.01$ and *** $p < 0.001$ referred to the control groups, Student's *t* tests.

treated with BBG displayed a selective decrease of *Casp1* among other inflammasome-associated genes (Fig. 7B). We also measured increased expression of M2-related *Mrc1*, *Arg1* and *Jak3* following BBG administration but no changes regarding M1-signature genes (Fig. 7B). On the other hand, treatment with JNJ-47965567 was associated to a significant down-regulation of *P2rx7* transcripts together with reductions in the expression of several M1 (*Cd86*, *Nos2* and *Ccl3*) but also M2 (*Stat6*) polarization markers (Fig. 7C). Overall, these observations suggest inhibitory effects of both drugs over centrally expressed P2x7 receptors leading to subtle modulation of inflammatory responses during recovery from cuprizone intoxication.

4. Discussion

P2x7 receptors have been described as an emerging target in CNS inflammatory diseases but their therapeutic potential in MS remains uncertain due to inconsistency among studies using EAE to model the disease. In this study, we evaluated the involvement of P2x7 receptors in the cuprizone model of toxic demyelination, which offers the opportunity to investigate the CNS processes of myelin degeneration and repair without the influence of the peripheral immune system, mimicking pattern III lesions in the brain of MS patients.

P2x7 receptor transcription was robustly upregulated during the time-course of cuprizone intoxication. We also found a prominent

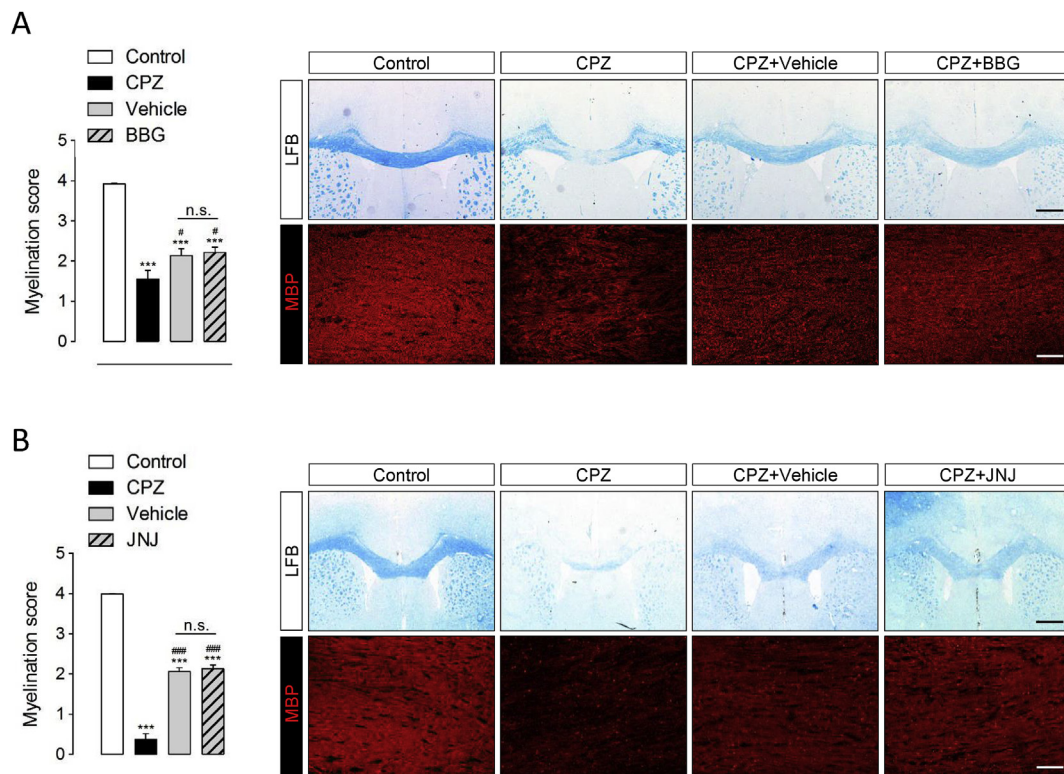


Fig. 6. Pharmacological blockade of P2x7 receptors does not improve spontaneous remyelination in the cuprizone model. Mice received cuprizone in the diet for 6 weeks and BBG (50 mg/Kg), JNJ-47965567 (JNJ; 30 mg/Kg) or vehicle solutions during a 2 week remyelination phase. (A, B) LFB and MBP immunostaining revealed extensive demyelination at 6 weeks of cuprizone administration and partial recovery 2 weeks after toxin withdrawal. Scoring of LFB and MBP staining showed no differences between mice treated with BBG (A), JNJ-47965567 (B) or vehicle during the recovery phase ($n = 4-6$ mice per group). *** $p < 0.0001$ control mice; # $p < 0.05$ and ### $p < 0.001$ versus mice treated with cuprizone for 6 weeks; One-way ANOVA followed by Newman-Keuls multiple comparison tests. Scale bars: 25 μ m. Scale bars: 500 μ m (LFB) and 50 μ m (MBP).

increase in P2x7 protein levels in brain homogenates and stronger P2x7-immunostaining in the corpus callosum at 6 weeks of cuprizone feeding. Demyelination and reactive gliosis occur at the highest levels at this time point thus appearing that increased P2x7 receptor levels in cuprizone model may be due to the expression of the protein by proliferating microglia and astrocytes. Despite both cell types expressed P2x7 receptors at some extent, analysis of confocal images suggested a preferential localization of the receptor on microglial cells in control and demyelinated corpus callosum. These observations are consistent with previous reports that astrocytes exhibit low levels of P2x7 receptors even in inflammatory degenerative conditions such as epilepsy, Alzheimer's or Huntington's disease (Díaz-Hernández et al., 2012; Díaz-Hernández et al., 2009; Jimenez-Pacheco et al., 2016). On the other hand, the pattern of P2x7 receptor modulation during the time-course of cuprizone administration might be also related, at least in part, to the localization of the protein in cells of the oligodendrocyte lineage. Experimental evidence shows that mature oligodendrocytes and OPCs express functionally active P2x7 receptors that mediate cell death *in vitro* and *in vivo* (Kaczmarek-Hajek et al., 2018; Matute et al., 2007; Wang et al., 2009; Zhang et al., 2014). In this regard, it is worth mentioning that P2x7 receptor expression is increased in the normal-appearing optic nerve of MS patients before lesion formation making oligodendrocytes more vulnerable to ATP excitotoxicity (Matute et al., 2007). Our results show a peak of P2x7 receptor transcriptional up-regulation at 3 weeks of cuprizone intoxication thus matching the time point of maximal oligodendrocyte apoptosis and repression of myelin genes in the model (Matsushima and Morell, 2001). In this context, it seems plausible to speculate that P2x7 receptors may contribute to cuprizone-induced apoptosis of oligodendroglial cells. Mechanistic considerations notwithstanding, the present results suggest that altered P2x7 receptor-mediated signaling participates

in the pathogenesis of primary demyelination.

Multiple lines of evidence point to a relevant pathogenic role for inflammasomes in MS and animal models of the disease (Barclay and Shinohara, 2017; Freeman et al., 2017). Yet, there is little evidence on the regulation of the inflammasomes during primary demyelination. In this study, induction of P2x7 receptors was paralleled by a robust up-regulation of the inflammasome-associated genes *Nlrp3*, *Asc* and *Il1b* in demyelinated tissue. Moreover, P2x7 deletion inhibited the expression of several NLRP3 genes thus implicating P2x7 receptors in inflammasome activation during cuprizone intoxication. Also concerning inflammatory responses, the induction of several pro-inflammatory cytokines involved in MS pathogenesis, including *Tnfa*, *Ccl2* and *Ccl3* (Conductier et al., 2010; Janssen et al., 2016; Pegoretti et al., 2018), was equally impaired in P2x7 receptor knockout mice. Together, these results show that P2x7 receptors contribute robustly to the inflammatory processes that cause demyelination. Indeed, a major finding in the present study is that P2x7 knockout reduces the severity of myelin degeneration by cuprizone feeding. In the context of previous studies, our findings strengthen the hypothesis that exacerbation of EAE symptomatology in P2x7 receptor null mice reflects the role of this protein in regulating the homeostasis of peripheral immune cells (Chen and Brosnan, 2006). Mechanistically, we hypothesized that the myelin protective phenotype of P2x7 receptor deficiency in the cuprizone model reflects blunted microglia-driven inflammation because these cells expressed high levels of P2x7 receptors and microglial cell numbers were significantly reduced in the demyelinated corpus callosum of P2x7 receptor knockout mice. Furthermore, P2x7 deletion was associated to lower numbers of microglial cells positive for the pro-inflammatory marker iNOS as well as to attenuated induction of M1-phenotype genes in demyelinated tissue. Altogether, these observations strongly suggest that P2x7 receptors drive

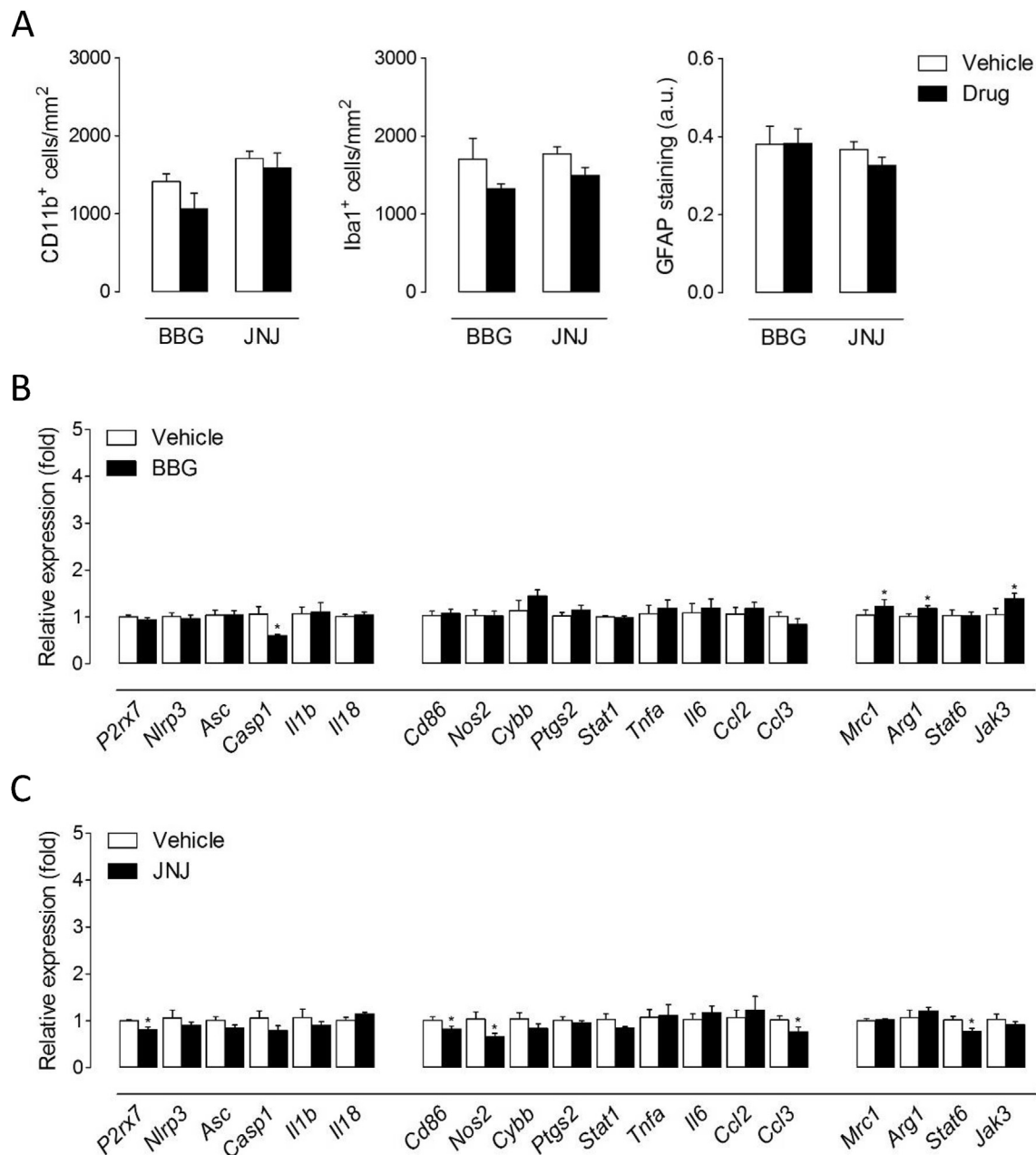


Fig. 7. Effect of P2x7 receptor antagonists on glial cells and inflammatory responses during remyelination. (A) Quantification of CD11b⁺ and Iba1⁺ cells and GFAP immunoreactivity following treatment with P2x7 receptor antagonists. Treatment with BBG or JNJ-47965567 during recovery from cuprizone intoxication did not modulate the presence of microglia/macrophages or astrocytes in remyelinating corpus callosum ($n = 5-6$ mice per group). (B, C) Expression of inflammasome- and polarization-related molecules assessed by RT-qPCR in brain tissue from mice treated with BBG (B) or JNJ-47965567 (C). Data represent fold change relative to vehicle-treated mice normalized to *Gapdh*, *Hprt1* and *Ppia* ($n = 5-6$ mice per group). * $p < 0.05$; Student's *t* tests.

microglia proliferation and/or functional polarization during cuprizone intoxication. While there is an established link between P2x7 receptor expression/function and the proliferation of microglia (Monif et al., 2009, 2016), its role as regulator of functional polarization of these cells has been poorly investigated. In this study, analysis of M1/2-phenotype markers in microglia purified using flow cytometry did not show significant differences between wild-type and P2x7 receptor null mice at 6 weeks of cuprizone intoxication. These results argue against the possibility that P2x7 receptors modulate the functional imprinting of microglia in severely demyelinated tissue, although regulatory roles at earlier time-points of the demyelination process cannot be excluded.

Mice lacking P2x7 receptors developed an attenuated astroglial reaction following cuprizone intoxication mimicking previous observations

in the EAE disease model (Sharp et al., 2008). However, the extent to which direct modulation of astrogliosis halts the progression of myelin injury or, conversely, occurs as a consequence of the reduced susceptibility to cuprizone induced demyelination of P2x7 receptor deficient mice, is uncertain. Indeed, the role of astrocytes in the cuprizone model is difficult to evaluate as both supportive and destructive functions have been described (Gudi et al., 2014). From a mechanistic perspective, our observation that these cells exhibit P2x7 receptors in injured white matter is consistent with previous reports in autopsy brain tissue from MS patients (Narcisse et al., 2005) and suggest that astrocytes might be direct targets of purinergic signaling during toxic demyelination, as proposed in studies from EAE mice (Grygorowicz et al., 2016; Sharp et al., 2008). Alternatively, the predominant expression of P2x7 receptors in activated

microglial cells supports the hypothesis that suppression of astrogliosis in P2x7 receptor null mice results from direct negative modulation of microglia pro-inflammatory functions. Indeed, the best understood effect of P2x7 receptor signaling in microglial cells is the production of IL-1 β by activated microglia (Giuliani et al., 2017) and both astrogliosis proliferation and P2x7 receptor expression by these cells are under the control of IL-1 β in neuroinflammatory conditions (Giuliani and Lachman, 1985; Narcisse et al., 2005). In all, our results are consistent with a model in which ATP produced during the time-course of demyelination activates P2x7 receptors in microglia and possibly astrocytes leading to IL-1 β release and subsequent proliferation of both pools of inflammatory cells.

Fostering remyelination is regarded as a promising therapeutic strategy for the treatment of all stages of MS (Kremer et al., 2015). The generation of new oligodendrocytes capable of repair is under the tight control of microglia/macrophages which contribute to remyelination by phagocytosis of myelin debris and by secreting signalling molecules that regulate OPC function either directly or acting via other cell types such as astrocytes (Kotter et al., 2005; Mason et al., 2001; Skripuletz et al., 2011). In particular, successful myelin regeneration is driven by a temporally limited inflammatory response controlled by a microglia/macrophage switch to a regenerative M2 activation state and inhibited by persistent M1 cytotoxic inflammation (Miron and Franklin, 2014). The relevance of this mechanism has been corroborated by recent observations that a shift in microglial polarization toward the beneficial M2 phenotype attenuates myelin pathology in the cuprizone model (Chen et al., 2014; Guglielmetti et al., 2016; Janssens et al., 2015). In this context, our findings that P2x7 receptor levels remain elevated following cuprizone withdrawal and that loss of P2x7 receptor function attenuates the accumulation of M1 phenotype microglia in demyelinated tissue prompted us to evaluate the efficacy of P2x7 receptor blockade to promote remyelination. Treatment with the P2x7 receptor inhibitors BBG and JNJ-47965567 was associated to subtle, drug-specific changes in the expression of inflammatory and microglia polarization related molecules. These apparent discrepancies most likely result from experimental differences concerning drug administration procedures that modulate the efficacy and selectivity of P2x7 receptor blockade *in vivo*. Regardless differences concerning the anti-inflammatory profile of each compound in remyelinating tissue, administration of either BBG or JNJ-47965567 failed to significantly enhance the repair of damaged myelin in the time-window analyzed in this study. There could be multiple reasons why we have observed a myelin protective phenotype in the P2x7 receptor knockout mice but an absence of any treatment effect with both P2x7 antagonists in the cuprizone model. In this regard, it is worth mentioning that BBG is a weak P2x7 receptor antagonist. On the other hand, JNJ-47965567 is a more potent and selective P2x7 antagonist but displays a short half-life in mice, which may result in insufficient daily exposure and pharmacological coverage at the P2x7 receptor. Treatment with both P2x7 antagonists was quite short in duration (2 weeks) after cuprizone challenge which might not be sufficient to see a treatment effect. Lastly, treatment with both P2x7 antagonists was initiated after the cuprizone challenge, which might be suboptimal and is certainly different to the situation with the P2x7 knockout mice that lack the receptor before starting the cuprizone challenge. These considerations notwithstanding, the failure of both antagonists to promote remyelination strongly suggest that blockade of P2x7 function is not able to limit lesion severity and engage myelin repair mechanism in a pre-existing inflammatory environment. These results are likely to reflect the complex role of purinergic P2x7 receptor signalling in regulating different pools of glial cells that orchestrate myelin repair. In this context, it is noteworthy that the decreased number of M1 microglial cells in demyelinated tissue of P2x7 receptor null mice was not associated to an increased presence of the M2 activation state. These results suggest that, while somehow contributing to the cytotoxic phenotype of these cells, P2x7 receptor signaling does not promote the crucial switch to regenerative microglia phenotypes in the cuprizone model. This hypothesis is further supported by the lack of significant differences concerning the expression of M2 polarization

markers in microglia purified from P2x7 receptor knockout mice at the time-point of maximal demyelination and incipient remyelination. On the other hand, a direct or indirect inhibition of astroglial reaction by P2x7 receptor blockade, as suggested by our results in *P2rx7* null mice, would equally influence the myelin repair capacity of these cells according to current knowledge in the model (Kanekiyo et al., 2013; Patel et al., 2012). Finally, the accumulation of NG2⁺ progenitors was not altered by P2x7 receptor deficiency, excluding the possibility that purinergic signaling directly modulates the OPCs recruitment or proliferation capacity through P2x7 receptors.

In conclusion, the findings presented here demonstrate that P2x7 receptors contribute to microglial and astrocytic responses toward myelin pathology, as evidenced by a reduced demyelination, glial reaction, presence of M1 microglia, and expression of pro-inflammatory molecules in P2x7 receptor knockout mice. However, our results also indicate that P2x7 receptors are not master regulators of microglia polarization in a demyelinating context and that pharmacological blockade of P2x7 receptors under a therapeutic regimen is inefficient to attenuate inflammation and promote the repair of degenerated myelin. Together, these results identify P2x7 receptors as mediators of primary demyelination and suggest potential applications but also limitations of the P2x7 receptor in supporting a recovery from more progressed pathological states.

Author contributions

AB-C carried out pharmacological treatments, gene expression and immunohistochemical studies and performed statistical analyses. AM and RC participated in flow cytometry and immunohistochemical experiments and carried out statistical analyses. IK supervised immunohistochemical experiments. SM conceived and designed the study, prepared the figures and drafted the manuscript. CM coordinated the study. All authors reviewed the manuscript.

Acknowledgements

AB-C and AM held fellowships from the Basque Government. This study was supported by grants from the Spanish Ministry of Economy and Competitiveness (SAF2016-75292-R to CM), CIBERNED (CB06/0005/0076 to CM), ISCIII (PI18/00513 to SM), Basque Government (IT1203-19 to CM and PIBA19-0059 to SM) and ARSEP Foundation (ARSEP16/01 to SM and CM). The authors are also grateful for the support of the postdoctoral research program of the Hungarian Academy of Sciences in later stages (to AB-C) and to the Momentum Program (LP2013-54/2013 to IK). The authors would like to thank Prof. Beáta Sperl gh for providing P2x7 knockout mice for preliminary anatomical experiments and Janssen Research & Development for providing JNJ-47965567.

Appendix A. Supplementary data

Supplementary data to this article can be found online at <https://doi.org/10.1016/j.bbih.2020.100062>.

References

- Adriouch, S., Hubert, S., Pechberty, S., Koch-Nolte, F., Haag, F., Seman, M., 2007. NAD⁺ released during inflammation participates in T cell homeostasis by inducing ART2-mediated death of naive T cells *in vivo*. *J. Immunol.* 179, 186–194.
- Aryanpour, R., Pasbakhsh, P., Zibara, K., Namjoo, Z., Beigi Boroujeni, F., Shahbeigi, S., Kashani, I.R., Beyer, C., Zendehele, A., 2017. Progesterone therapy induces an M1 to M2 switch in microglia phenotype and suppresses NLRP3 inflammasome in a cuprizone-induced demyelination mouse model. *Int. Immunopharm.* 51, 131–139.
- Aswad, F., Kawamura, H., Dennert, G., 2005. High sensitivity of CD4⁺CD25⁺ regulatory T cells to extracellular metabolites nicotinamide adenine dinucleotide and ATP: a role for P2X7 receptors. *J. Immunol.* 175, 3075–3083.
- Barclay, W., Shinohara, M.L., 2017. Inflammasome activation in multiple sclerosis and experimental autoimmune encephalomyelitis (EAE). *Brain Pathol.* 27, 213–219.

- Baricordi, O.R., Melchiorri, L., Adinolfi, E., Falzoni, S., Chiozzi, P., Buell, G., Di Virgilio, F., 1999. Increased proliferation rate of lymphoid cells transfected with the P2X₇(7) ATP receptor. *J. Biol. Chem.* 274, 33206–33208.
- Barnett, M.H., Prineas, J.W., 2004. Relapsing and remitting multiple sclerosis: pathology of the newly forming lesion. *Ann. Neurol.* 55, 458–468.
- Bernal-Chico, A., Canedo, M., Manterola, A., Victoria Sánchez-Gómez, M., Pérez-Samartín, A., Rodríguez-Puertas, R., Matute, C., Mato, S., 2015. Blockade of monoacylglycerol lipase inhibits oligodendrocyte excitotoxicity and prevents demyelination in vivo. *Glia* 63, 163–176.
- Bhattacharya, A., Wang, Q., Ao, H., Shoblock, J.R., Lord, B., Aluisio, L., Fraser, I., Nepomuceno, D., Neff, R.A., Welty, N., Lovenberg, T.W., Bonaventure, P., Wickenden, A.D., Letavic, M.A., 2013. Pharmacological characterization of a novel centrally permeable P2X₇ receptor antagonist: JNJ-47965567. *Br. J. Pharmacol.* 170, 624–640.
- Brough, D., Le Feuvre, R.A., Iwakura, Y., Rothwell, N.J., 2002. Purinergic (P2X₇) receptor activation of microglia induces cell death via an interleukin-1-independent mechanism. *Mol. Cell. Neurosci.* 19, 272–280.
- Chen, L., Brosnan, C.F., 2006. Exacerbation of experimental autoimmune encephalomyelitis in P2X₇R^{-/-} mice: evidence for loss of apoptotic activity in lymphocytes. *J. Immunol.* 176, 3115–3126.
- Chen, S., Zhang, H., Pu, H., Wang, G., Li, W., Leak, R.K., Chen, J., Liou, A.K., Hu, X., 2014. n-3 PUFA supplementation benefits microglial responses to myelin pathology. *Sci. Rep.* 4, 7458.
- Chu, F., Shi, M., Zheng, C., Shen, D., Zhu, J., Zheng, X., Cui, L., 2018. The roles of macrophages and microglia in multiple sclerosis and experimental autoimmune encephalomyelitis. *J. Neuroimmunol.* 318, 1–7.
- Compston, A., Coles, A., 2008. Multiple sclerosis. *Lancet* 372, 1502–1517.
- Conductier, G., Blondeau, N., Guyon, A., Nahon, J.L., Rovère, C., 2010. The role of monocyte chemoattractant protein MCP1/CCL2 in neuroinflammatory diseases. *J. Neuroimmunol.* 224, 93–100.
- Díaz-Hernández, J.I., Gómez-Villafuertes, R., León-Otegui, M., Hontecillas-Prieto, L., Del Puerto, A., Trejo, J.L., Lucas, J.J., Garrido, J.J., Gualix, J., Miras-Portugal, M.T., Díaz-Hernández, M., 2012. In vivo P2X₇ inhibition reduces amyloid plaques in Alzheimer's disease through GSK3 β and secretases. *Neurobiol. Aging* 33, 1816–1828.
- Duan, C., Liu, Y., Li, Y., Chen, H., Liu, X., Chen, X., Yue, J., Zhou, X., Yang, J., 2018. Sulfasalazine alters microglia phenotype by competing endogenous RNA effect of miR-136-5p and long non-coding RNA HOTAIR in cuprizone-induced demyelination. *Biochem. Pharmacol.* 155, 110–123.
- Díaz-Hernández, M., Díez-Zaera, M., Sánchez-Nogueiro, J., Gómez-Villafuertes, R., Canals, J.M., Alberch, J., Miras-Portugal, M.T., Lucas, J.J., 2009. Altered P2X₇-receptor level and function in mouse models of Huntington's disease and therapeutic efficacy of antagonist administration. *Faseb. J.* 23, 1893–1906.
- Freeman, L., Guo, H., David, C.N., Brickey, W.J., Jha, S., Ting, J.P., 2017. NLR members NLR4 and NLRP3 mediate sterile inflammasome activation in microglia and astrocytes. *J. Exp. Med.* 214, 1351–1370.
- Giulian, D., Lachman, L.B., 1985. Interleukin-1 stimulation of astroglial proliferation after brain injury. *Science* 228, 497–499.
- Giuliani, A.L., Sarti, A.C., Falzoni, S., Di Virgilio, F., 2017. The P2X₇ receptor-interleukin-1 liaison. *Front. Pharmacol.* 8, 123.
- Grygorowicz, T., Sulejczak, D., Struzynska, L., 2011. Expression of purinergic P2X₇ receptor in rat brain during the symptomatic phase of experimental autoimmune encephalomyelitis and after recovery of neurological deficits. *Acta Neurobiol. Exp.* 71, 65–73.
- Grygorowicz, T., Welnia-Kamińska, M., Struzynska, L., 2016. Early P2X₇R-related astrogliosis in autoimmune encephalomyelitis. *Mol. Cell. Neurosci.* 74, 1–9.
- Gu, B.J., Field, J., Duterte, S., Ou, A., Kilpatrick, T.J., Lechner-Scott, J., Scott, R., Lea, R., Taylor, B.V., Stankovich, J., Butzkueven, H., Gresle, M., Laws, S.M., Petrou, S., Hoffjan, S., Akkad, D.A., Graham, C.A., Hawkins, S., Glaser, A., Bedri, S.K., Hillert, J., Matute, C., Antiguada, A., Wiley, J.S., Consortium, A., 2015. A rare P2X₇ variant Arg307Gln with absent pore formation function protects against neuroinflammation in multiple sclerosis. *Hum. Mol. Genet.* 24, 5644–5654.
- Gudi, V., Gingele, S., Skripuletz, T., Stangel, M., 2014. Glial response during cuprizone-induced de- and remyelination in the CNS: lessons learned. *Front. Cell. Neurosci.* 8, 73.
- Guglielmetti, C., Le Blon, D., Santermans, E., Salas-Perdomo, A., Daans, J., De Vocht, N., Shah, D., Hoornaert, C., Praet, J., Peerlings, J., Kara, F., Bigot, C., Mai, Z., Goossens, H., Hens, N., Hendrix, S., Verhoye, M., Planas, A.M., Berneman, Z., van der Linden, A., Ponsaerts, P., 2016. Interleukin-13 immune gene therapy prevents CNS inflammation and demyelination via alternative activation of microglia and macrophages. *Glia* 64, 2181–2200.
- He, Y., Taylor, N., Fourgeaud, L., Bhattacharya, A., 2017. The role of microglial P2X₇: modulation of cell death and cytokine release. *J. Neuroinflammation* 14, 135.
- Henderson, A.P., Barnett, M.H., Parratt, J.D., Prineas, J.W., 2009. Multiple sclerosis: distribution of inflammatory cells in newly forming lesions. *Ann. Neurol.* 66, 739–753.
- Hu, X., Leak, R.K., Shi, Y., Suenaga, J., Gao, Y., Zheng, P., Chen, J., 2015. Microglial and macrophage polarization-new prospects for brain repair. *Nat. Rev. Neurol.* 11, 56–64.
- Humphreys, B.D., Rice, J., Kertesz, S.B., Dubyak, G.R., 2000. Stress-activated protein kinase/JNK activation and apoptotic induction by the macrophage P2X₇ nucleotide receptor. *J. Biol. Chem.* 275, 26792–26798.
- Idzko, M., Ferrari, D., Eltzschig, H.K., 2014. Nucleotide signalling during inflammation. *Nature* 509, 310–317.
- Janssen, K., Rickert, M., Clarner, T., Beyer, C., Kipp, M., 2016. Absence of CCL2 and CCL3 ameliorates central nervous system grey matter but not white matter demyelination in the presence of an intact blood-brain barrier. *Mol. Neurobiol.* 53, 1551–1564.
- Janssens, K., Maheshwari, A., Van den Haute, C., Baekelandt, V., Stinissen, P., Hendriks, J.J., Slaets, H., Hellings, N., 2015. Oncostatin M protects against demyelination by inducing a protective microglial phenotype. *Glia* 63, 1729–1737.
- Jiang, L.H., Mackenzie, A.B., North, R.A., Surprenant, A., 2000. Brilliant blue G selectively blocks ATP-gated rat P2X₇(7) receptors. *Mol. Pharmacol.* 58, 82–88.
- Jimenez-Pacheco, A., Diaz-Hernandez, M., Arribas-Blázquez, M., Sanz-Rodríguez, A., Olivos-Oré, L.A., Artalejo, A.R., Alves, M., Letavic, M., Miras-Portugal, M.T., Conroy, R.M., Delanty, N., Farrell, M.A., O'Brien, D.F., Bhattacharya, A., Engel, T., Henshall, D.C., 2016. Transient P2X₇ receptor antagonism produces lasting reductions in spontaneous seizures and gliosis in experimental temporal lobe epilepsy. *J. Neurosci.* 36, 5920–5932.
- Jun, D.J., Kim, J., Jung, S.Y., Song, R., Noh, J.H., Park, Y.S., Ryu, S.H., Kim, J.H., Kong, Y.Y., Chung, J.M., Kim, K.T., 2007. Extracellular ATP mediates necrotic cell swelling in SN4741 dopaminergic neurons through P2X₇ receptors. *J. Biol. Chem.* 282, 37350–37358.
- Kaczmarek-Hajek, K., Zhang, J., Kopp, R., Grosche, A., Rissiek, B., Saul, A., Bruzzone, S., Engel, T., Jooss, T., Krautloher, A., Schuster, S., Magnus, T., Stadelmann, C., Sirkko, S., Koch-Nolte, F., Eulenburg, V., Nicke, A., 2018. Re-evaluation of neuronal P2X₇ expression using novel mouse models and a P2X₇-specific nanobody. *Elife* 7.
- Kanekiyo, K., Inamori, K., Kitazume, S., Sato, K., Maeda, J., Higuchi, M., Kizuka, Y., Korekane, H., Matsuo, I., Honke, K., Taniguchi, N., 2013. Loss of branched O-mannosyl glycans in astrocytes accelerates remyelination. *J. Neurosci.* 33, 10037–10047.
- Kawamura, H., Aswad, F., Minagawa, M., Malone, K., Kaslow, H., Koch-Nolte, F., Schott, W.H., Leiter, E.H., Dennert, G., 2005. P2X₇ receptor-dependent and -independent T cell death is induced by nicotinamide adenine dinucleotide. *J. Immunol.* 174, 1971–1979.
- Koch-Henriksen, N., Sorensen, P.S., 2010. The changing demographic pattern of multiple sclerosis epidemiology. *Lancet Neurol.* 9, 520–532.
- Kotter, M.R., Zhao, C., van Rooijen, N., Franklin, R.J., 2005. Macrophage-depletion induced impairment of experimental CNS remyelination is associated with a reduced oligodendrocyte progenitor cell response and altered growth factor expression. *Neurobiol. Dis.* 18, 166–175.
- Kremer, D., Küry, P., Dutta, R., 2015. Promoting remyelination in multiple sclerosis: current drugs and future prospects. *Mult. Scler.* 21, 541–549.
- Le Blon, D., Guglielmetti, C., Hoornaert, C., Quarta, A., Daans, J., Dooley, D., Lemmens, E., Praet, J., De Vocht, N., Reekmans, K., Santermans, E., Hens, N., Goossens, H., Verhoye, M., Van der Linden, A., Berneman, Z., Hendrix, S., Ponsaerts, P., 2016. Intracerebral transplantation of interleukin 13-producing mesenchymal stem cells limits microgliosis, oligodendrocyte loss and demyelination in the cuprizone mouse model. *J. Neuroinflammation* 13, 288.
- Lucchinetti, C., Brück, W., Parisi, J., Scheithauer, B., Rodríguez, M., Lassmann, H., 2000. Heterogeneity of multiple sclerosis lesions: implications for the pathogenesis of demyelination. *Ann. Neurol.* 47, 707–717.
- Mahad, D., Ziabreva, I., Lassmann, H., Turnbull, D., 2008. Mitochondrial defects in acute multiple sclerosis lesions. *Brain* 131, 1722–1735.
- Manterola, A., Bernal-Chico, A., Cipriani, R., Canedo-Antelo, M., Moreno-García, Á., Martín-Fontecha, M., Pérez-Cerdá, F., Sánchez-Gómez, M.V., Ortega-Gutiérrez, S., Brown, J.M., Hsu, K.L., Cravatt, B., Matute, C., Mato, S., 2018. Deregulation of the endocannabinoid system and therapeutic potential of ABHD6 blockade in the cuprizone model of demyelination. *Biochem. Pharmacol.* 157, 189–201.
- Mason, J.L., Suzuki, K., Chaplin, D.D., Matsushima, G.K., 2001. Interleukin-1 β promotes repair of the CNS. *J. Neurosci.* 21, 7046–7052.
- Matsushima, G.K., Morell, P., 2001. The neurotoxicant, cuprizone, as a model to study demyelination and remyelination in the central nervous system. *Brain Pathol.* 11, 107–116.
- Matute, C., Torre, I., Pérez-Cerdá, F., Pérez-Samartín, A., Alberdi, E., Ettxebarria, E., Arranz, A.M., Ravid, R., Rodríguez-Antigüedad, A., Sánchez-Gómez, M., Domercq, M., 2007. P2X₇(7) receptor blockade prevents ATP excitotoxicity in oligodendrocytes and ameliorates experimental autoimmune encephalomyelitis. *J. Neurosci.* 27, 9525–9533.
- Miron, V.E., Boyd, A., Zhao, J.W., Yuen, T.J., Ruckh, J.M., Shadrach, J.L., van Wijngaarden, P., Wagers, A.J., Williams, A., Franklin, R.J., ffrench-Constant, C., 2013. M2 microglia and macrophages drive oligodendrocyte differentiation during CNS remyelination. *Nat. Neurosci.* 16, 1211–1218.
- Miron, V.E., Franklin, R.J., 2014. Macrophages and CNS remyelination. *J. Neurochem.* 130, 165–171.
- Monif, M., Reid, C.A., Powell, K.L., Drummond, K.J., O'Brien, T.J., Williams, D.A., 2016. Interleukin-1 β has trophic effects in microglia and its release is mediated by P2X₇R pore. *J. Neuroinflammation* 13, 173.
- Monif, M., Reid, C.A., Powell, K.L., Smart, M.L., Williams, D.A., 2009. The P2X₇ receptor drives microglial activation and proliferation: a trophic role for P2X₇R pore. *J. Neurosci.* 29, 3781–3791.
- Narcisse, L., Scemes, E., Zhao, Y., Lee, S.C., Brosnan, C.F., 2005. The cytokine IL-1 β transiently enhances P2X₇ receptor expression and function in human astrocytes. *Glia* 49, 245–258.
- Oyanguren-Desez, O., Rodríguez-Antigüedad, A., Villoslada, P., Domercq, M., Alberdi, E., Matute, C., 2011. Gain-of-function of P2X₇ receptor gene variants in multiple sclerosis. *Cell Calcium* 50, 468–472.
- Patel, J.R., Williams, J.L., Muccigrosso, M.M., Liu, L., Sun, T., Rubin, J.B., Klein, R.S., 2012. Astrocyte TNFR2 is required for CXCL12-mediated regulation of oligodendrocyte progenitor proliferation and differentiation within the adult CNS. *Acta Neuropathol.* 124, 847–860.
- Patrikios, P., Stadelmann, C., Kutzelnigg, A., Rauschka, H., Schmidbauer, M., Laursen, H., Sorensen, P.S., Brück, W., Lucchinetti, C., Lassmann, H., 2006. Remyelination is extensive in a subset of multiple sclerosis patients. *Brain* 129, 3165–3172.

- Paxinos, G., Franklin, K., 2012. *The Mouse Brain in Stereotaxic Coordinates*. Academic Press.
- Pegoretti, V., Baron, W., Laman, J.D., Eisel, U.L.M., 2018. Selective modulation of TNF-TNFRs signaling: insights for multiple sclerosis treatment. *Front. Immunol.* 9, 925.
- Peng, W., Cotrina, M.L., Han, X., Yu, H., Bekar, L., Blum, L., Takano, T., Tian, G.F., Goldman, S.A., Nedergaard, M., 2009. Systemic administration of an antagonist of the ATP-sensitive receptor P2X7 improves recovery after spinal cord injury. *Proc. Natl. Acad. Sci. U. S. A.* 106, 12489–12493.
- Sharp, A.J., Polak, P.E., Simonini, V., Lin, S.X., Richardson, J.C., Bongarzone, E.R., Feinstein, D.L., 2008. P2x7 deficiency suppresses development of experimental autoimmune encephalomyelitis. *J. Neuroinflammation* 5, 33.
- Skripuletz, T., Gudi, V., Hackstette, D., Stangel, M., 2011. De- and remyelination in the CNS white and grey matter induced by cuprizone: the old, the new, and the unexpected. *Histol. Histopathol.* 26, 1585–1597.
- Sperlágh, B., Illes, P., 2014. P2X7 receptor: an emerging target in central nervous system diseases. *Trends Pharmacol. Sci.* 35, 537–547.
- Sperlágh, B., Vizi, E.S., Wirkner, K., Illes, P., 2006. P2X7 receptors in the nervous system. *Prog. Neurobiol.* 78, 327–346.
- Szulzewsky, F., Pelz, A., Feng, X., Synowitz, M., Markovic, D., Langmann, T., Holtman, I.R., Wang, X., Eggen, B.J., Boddeke, H.W., Hambardzumyan, D., Wolf, S.A., Kettenmann, H., 2015. Glioma-associated microglia/macrophages display an expression profile different from M1 and M2 polarization and highly express Gpnmb and Spp1. *PLoS One* 10, e0116644.
- Trapp, B.D., Nave, K.A., 2008. Multiple sclerosis: an immune or neurodegenerative disorder? *Annu. Rev. Neurosci.* 31, 247–269.
- Wang, L.Y., Cai, W.Q., Chen, P.H., Deng, Q.Y., Zhao, C.M., 2009. Downregulation of P2X7 receptor expression in rat oligodendrocyte precursor cells after hypoxia ischemia. *Glia* 57, 307–319.
- WHO, 1970. Specifications for the Identity and Purity of Food Additives and Their Toxicological Evaluation: Some Food Colours, Emulsifiers, Stabilizers, Anticaking Agents, and Certain Other Substances. Report on the Joint FAO-WHO Expert Committee on Food Additives, Rome, 27 May–4 June 1969. World Health Organ Tech Rep Ser, pp. 1–36.
- Witting, A., Chen, L., Cudaback, E., Straiker, A., Walter, L., Rickman, B., Möller, T., Brosnan, C., Stella, N., 2006. Experimental autoimmune encephalomyelitis disrupts endocannabinoid-mediated neuroprotection. *Proc. Natl. Acad. Sci. U. S. A.* 103, 6362–6367.
- Yip, L., Woehrle, T., Corriden, R., Hirsh, M., Chen, Y., Inoue, Y., Ferrari, V., Insel, P.A., Junger, W.G., 2009. Autocrine regulation of T-cell activation by ATP release and P2X7 receptors. *Faseb. J.* 23, 1685–1693.
- Yu, Z., Sun, D., Feng, J., Tan, W., Fang, X., Zhao, M., Zhao, X., Pu, Y., Huang, A., Xiang, Z., Cao, L., He, C., 2015. MSX3 switches microglia polarization and protects from inflammation-induced demyelination. *J. Neurosci.* 35, 6350–6365.
- Zhang, Y., Chen, K., Sloan, S.A., Bennett, M.L., Scholze, A.R., O'Keeffe, S., Phatnani, H.P., Guarnieri, P., Caneda, C., Ruderisch, N., Deng, S., Liddelow, S.A., Zhang, C., Daneman, R., Maniatis, T., Barres, B.A., Wu, J.Q., 2014. An RNA-sequencing transcriptome and splicing database of glia, neurons, and vascular cells of the cerebral cortex. *J. Neurosci.* 34, 11929–11947.